Journal of Organometallic Chemistry 695 (2010) 1682–1687

Contents lists available at ScienceDirect

Journal of Organometallic Chemistry

journal homepage: www.elsevier.com/locate/jorganchem

Theoretical study on ligand exchange reaction mechanisms of iron(IV) complexes with two different group 14 element ligands, $Cp(CO)FeH(EEt_3)(E'Et_3)$ with $(HEEt_3)$ (E, E′ = Si, Ge, Sn)

Xiangai Yuan, Siwei Bi*, Lingjun Liu, Min Sun, Jiayong Wang

College of Chemistry and Chemical Engineering, Qufu Normal University, Qufu, Shandong 273165, China

ARTICLE INFO

Article history:
Received 8 February 2010
Received in revised form
11 March 2010
Accepted 23 March 2010
Available online 21 April 2010

Keywords:
DFT
Fe(IV) complex
Ligand exchange

ABSTRACT

A computational study with Becke3LYP of DFT was carried out to investigate the ligand exchange reaction mechanisms of $Cp(CO)FeH(EEt_3)(E'Et_3)$ with $(HEEt_3)$ (E, E′ = Si, Ge, Sn). The full ligand exchange reactions were computed, starting from the reductive elimination and then followed by the oxidative addition. The reductive elimination of $HEEt_3$ from the Fe(IV) center takes place more readily in the order $Et_3Si{-}H > Et_3Ge{-}H \gg Et_3Sn{-}H$. There are several reasons for the order: (i) the thermodynamic stability of the corresponding products, (ii) the order of bond binding energy: $Et_3Si{-}H > Et_3Ge{-}H > Et_3Sn{-}H$, (iii) the order of the interaction of E–H: $Et_3Si{-}H > Et_3Ge{-}H > Et_3Sn{-}H$.

© 2010 Elsevier B.V. All rights reserved.

1. Introduction

Iron is known to play an active role in the catalytic cycles of many metalloenzymes and is the most prominent transition metal in biological systems [1]. So far, the most common oxidation states of iron in proteins are the +2 and +3, and higher oxidation states (+4 and +5) are often proposed for specific intermediates. Iron complexes with two group 14 element ligands are the key intermediates in the catalytic addition of E–E′ bonds (E, E′ = Si, Ge, Sn) to unsaturated organic molecules [2–9], such as catalytic addition of germylstannanes to alkynes [10–14].

Iron complexes having two same group 14 element ligands, such as $(C_5R_5)(CO)FeH(ER_3)_2$ (E = Si [15–26], Sn [27–30]), have been reported. Whereas, iron complexes having two different group 14 element ligands are little (only one $Cp(CO)FeH(SiPh_3)(SnPh_3)$) [31], though such complexes are quite limited and have the possibility of constructing an E–E′ bond. In 2009, H. Nakazawa et al. first gave a series of Fe(IV) complexes ($Cp(CO)FeH(EEt_3)(E'Et_3)$) with two different group 14 element ligands in good to high yields and studied their exchange reactions with $HEEt_3$ (E, E′ = Si, Ge, Sn) (see eqs. (1)–(5)), which involved first reductive elimination and following oxidative addition [32]. The results show that reductive elimination of $HEEt_3$ from the Fe(IV) center takes place more readily in the order $Et_3Si{-}H > Et_3Ge{-}H \gg Et_3Sn{-}H$.

To our knowledge, a few theoretical studies on iron complexes with two group 14 element ligands have been reported [26,33–36], but studies on Fe(IV) complexes with two different group 14 element ligands ($Cp(CO)FeH(EEt_3)(E'Et_3)$) have not been reported to date. In this work, our goal is to investigate the mechanisms of the exchange reactions and explore why the elimination of $HEEt_3$ from the Fe(IV) center takes place more readily in the order $Et_3Si{-}H > Et_3Ge{-}H \gg Et_3Sn{-}H$. We hope this study could provide further understanding for such kind of reactions and play a guiding role for further designing such kind of new reactions.

2. Computational details

Molecular geometries of all the complexes studied were optimized at the Becke3LYP level of density functional theory [37–40]. Frequency calculations at the same level of theory were also performed to identify all the stationary points as minima (zero imaginary frequencies) or transition states (one imaginary frequency) and to provide free energies at 333 K. The intrinsic reaction coordinate (IRC) [41,42] analysis was carried out to confirm that all stationary points are smoothly connected to each other. The lanl2dz basis set [43] including a double-ζ valence basis set with the Hay

* Corresponding author. Fax: +86 537 4456305.
E-mail address: siweibi@126.com (S. Bi).

0022-328X/$ – see front matter © 2010 Elsevier B.V. All rights reserved.
doi:10.1016/j.jorganchem.2010.03.028

and Wadt effective core potential (ECP) [44,45] was used for Fe, Si, Ge and Sn atoms and the 6-31G [46] basis set was used for other atoms. Polarization functions were selectively added for carbonyl C and O [C ($\zeta_d = 0.8$) and O ($\zeta_d = 0.8$)], H atoms directly connected to Fe atom [$\zeta_p = 0.11$], and Si, Ge, Sn atoms [Si ($\zeta_d = 0.262$), Ge ($\zeta_d = 0.246$) and Sn ($\zeta_d = 0.183$)]. All the DFT calculations were performed with Gaussian 03 packages [47].

Fig. 1 shows the key optimized structures with selected structural parameters for the species involved in the ligand exchange reactions (eqs. (1)–(5)). Computed structural parameters of **R1**, **Int2** and **P2** and the corresponding X-ray crystalline diffraction data (in parenthesis) are given. It is found that the calculated structural parameters are in well agreement with the X-ray crystalline diffraction data. Thus it can be confirmed that the basis sets are adequate for present study.

In Fig. 2 the calculated relative free energies (kcal/mol) and electronic energies (kcal/mol, in parentheses) are presented. The free energies and electronic energies differ significantly in cases where the number of reactant and product molecules is different for one-to-two or two-to-one transformations because of the entropic contribution. In this paper, relative free energies are used to analyze the reaction mechanisms. It should be noted here that the entropic contribution to the free energies based on the gas-phase calculations is overestimated for those steps involving substrate association or dissociation. Recent discussions on the overestimation can be found in the literature [48,49].

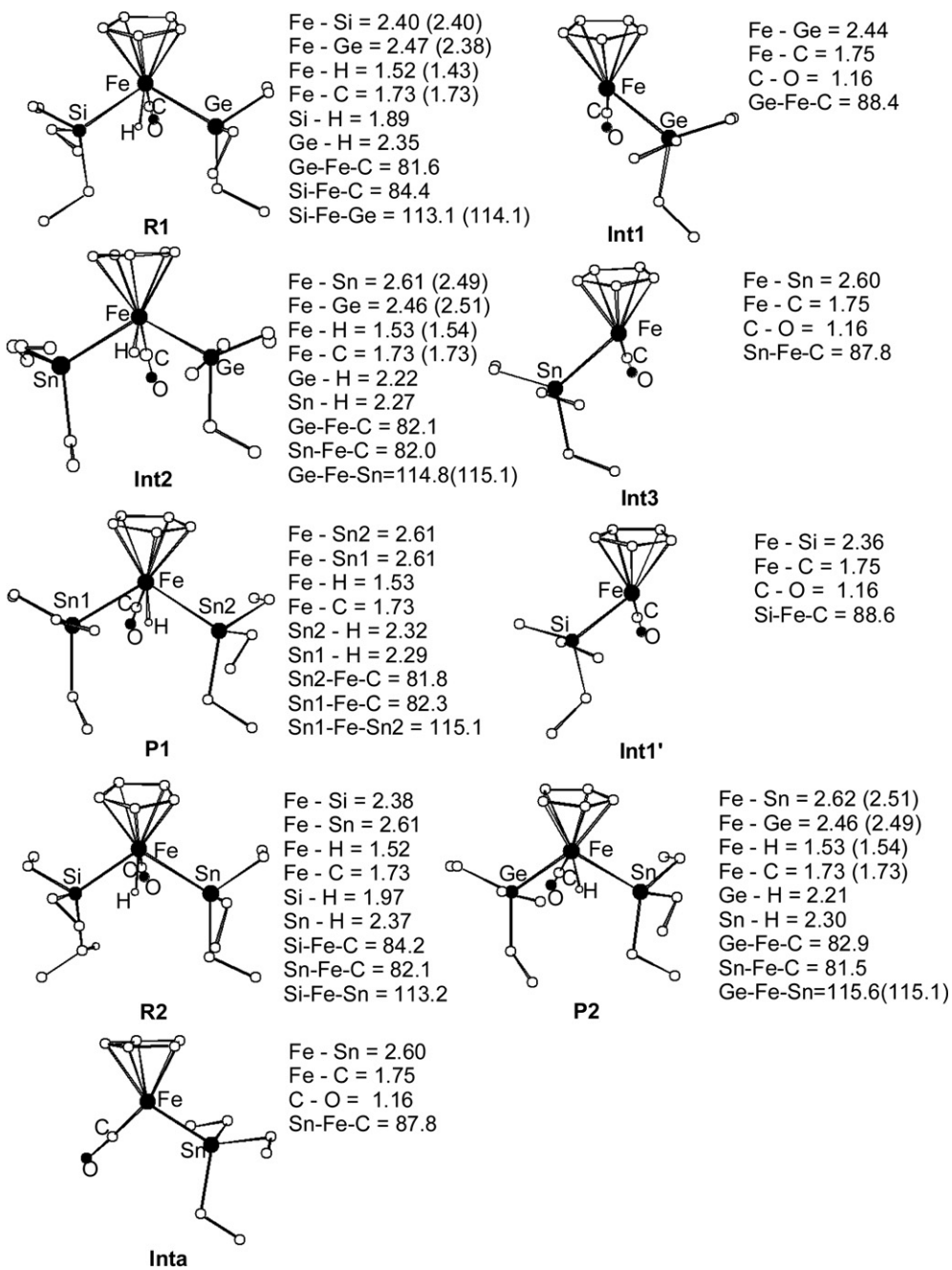

Fig. 1. Selected B3LYP optimized structures involved in the ligand exchange reaction together with selected bond distances and bond angles. The bond distances are given in Å. In **R1**, **Int2** and **P2**, the X-ray crystalline diffraction data of the original compound are given in parenthesis.

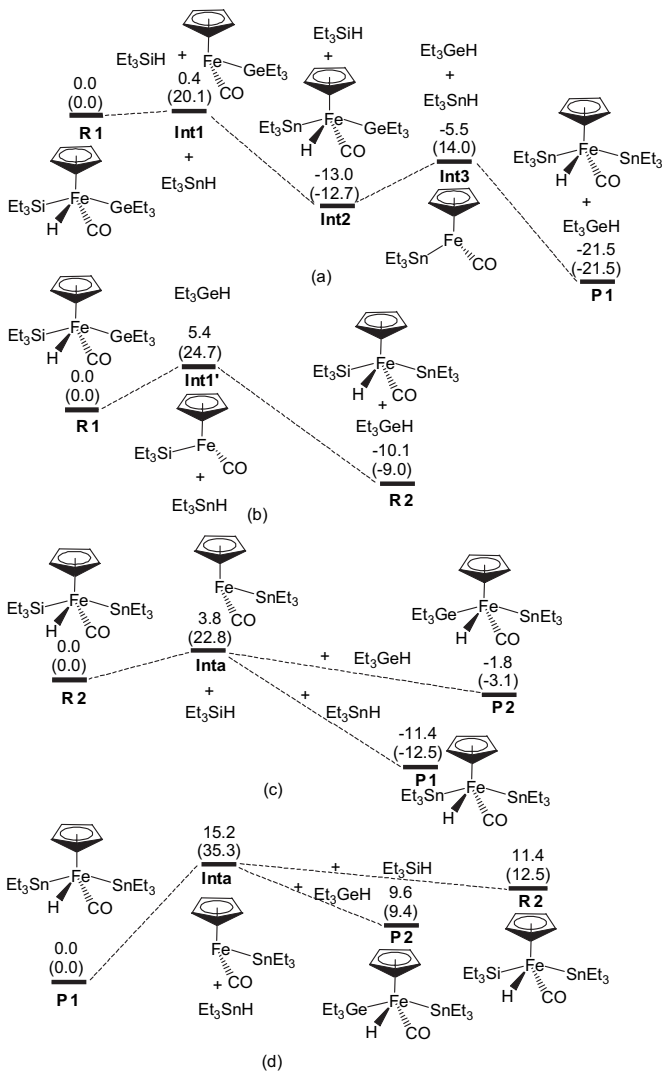

Fig. 2. Energy profile calculated for the eqs. (1)–(5). The relative free energies and electronic energies (in parentheses) are given in kcal/mol.

3. Results and discussions

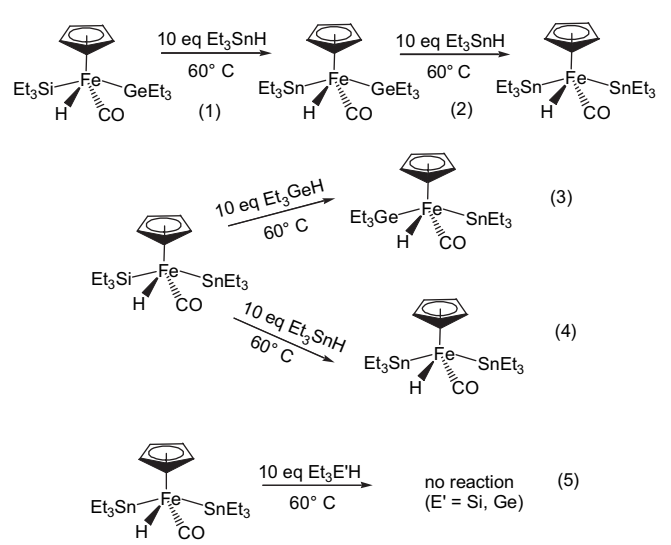

Very recently, H. Nakazawa and co-workers studied a series of the ligand exchange reactions of $Cp(CO)FeH(EEt_3)(E'Et_3)$ with $HEEt_3$ (E, E′ = Si, Ge, Sn) as shown in eqs. (1)–(5). The ligand exchange reaction consists of the reductive elimination and the following oxidative addition of $HEEt_3$. The reductive elimination of $HEEt_3$ from the Fe(IV) center takes place more readily in the order $Et_3Si{-}H > Et_3Ge{-}H \gg Et_3Sn{-}H$. H. Nakazawa et al. predicted that the reasons for the order were the bond energies of the both Fe–E and H–E, and the activation energies for the reductive elimination of $HEEt_3$ from the Fe(IV) center. But the related data and further theoretical investigations for the order have not been reported to date.

Another important issue needed to be addressed is that the reactions of $Cp(CO)FeH(SnEt_3)(SnEt_3)$ with $Et_3E'H$ (E = Si, Ge) cannot be observed. In this work, we attempt to investigate the mechanisms of the ligand exchange reactions in detail and address the two important issues mentioned above.

3.1. Reaction mechanisms of $Cp(CO)FeH(SiEt_3)(GeEt_3)$ with $Et_3Sn{-}H$ (eqs. (1) and (2))

The ligand exchange reactions of $Cp(CO)FeH(SiEt_3)(GeEt_3)$ (**R1**) with $Et_3Sn{-}H$ (eqs. (1) and (2)) are proposed to undergo two processes (Fig. 2(a)). The first process is the exchange of $SiEt_3$ for $SnEt_3$ to give a 18e $Cp(CO)FeH(SnEt_3)(GeEt_3)$ (**Int2**), which has been isolated experimentally by H. Nakazawa and co-workers [32]. Two steps are involved in the process. The first step is reductive elimination of $Et_3Si{-}H$ from **R1**, leading to bond cleavage of Fe–Si and Fe–H, and bond formation of Si–H. Instead, the reaction cannot be carried out through the reductive elimination of $Et_3Ge{-}H$ from **R1**, leading to bond cleavage of Fe–Ge and Fe–H and bond formation of Ge–H. The reductive elimination from **R1** could occur at either Fe–Si and Fe–H or Fe–Ge and Fe–H. We first calculated the bond dissociation energies of Fe–Si and Fe–Ge (Fig. 3(a)) and the binding energies of $Et_3Si{-}H$ and $Et_3Ge{-}H$. The results show the Fe–Si bond (dissociation energy: 35.5 kcal/mol) is stronger than the Fe–Ge (dissociation energy: 31.6 kcal/mol) bond. The difference in the bond dissociation energies is expectable, as generally believed that the Fe–Ge bond cleavage is more facile than the Fe–Si bond. Interestingly, the reductive elimination observed by H. Nakazawa et al. in eq. (1) cleaves the stronger bond rather than the weaker one. Whereas, the Si–H binding energy ($Et_3Si + H \rightarrow Et_3Si{-}H$) is calculated to be −95.5 kcal/mol and Ge–H binding energy ($Et_3Ge + H \rightarrow Et_3Ge{-}H$) is to be −88.0 kcal/mol, indicating $Et_3Si{-}H$ is more stable than $Et_3Ge{-}H$. The difference of binding energy (7.5 kcal/mol) suggests that reductive elimination of $Et_3Si{-}H$ from **R1** is more favorable than $Et_3Ge{-}H$.

The calculated potential energy profile for the reductive elimination of $Et_3Si{-}H$ from **R1** is illustrated in Fig. 2(a). The reductive elimination of $Et_3Si{-}H$ from **R1** to give **Int1** is barrierless, as can be verified from the always increasing relative energy of **R1** with decreasing Si–H bond distance in **R1** (see curve1 in Fig. 4). Similarly, the transformations from **Int2** to **Int3** (Fig. 2(a)), **R1** to **Int1′** (Fig. 2(b)), **R2** to **Inta** (Fig. 2(c)) and **P1** to **Inta** (Fig. 2(d)), are all barrierless (see curves 3, 4, 2 and 5 in Fig. 4, respectively).

The reductive elimination of $Et_3Si{-}H$ from **R1** gives the 16e species $Cp(CO)Fe(GeEt_3)$ (**Int1**) with a low free energy of 0.4 kcal/mol (see Fig. 2(a)), which is more stable than the **Int1′** obtained through the reductive elimination of $Et_3Ge{-}H$ from **R1** with a free energy of 5.4 kcal/mol (see Fig. 2(b)). Moreover, the subsequent oxidative addition of $Et_3Sn{-}H$ to **Int1** to afford $Cp(CO)FeH(SnEt_3)(GeEt_3)$ (**Int2**) with a low free energy of −13.0 kcal/mol, which is more stable than **R2** obtained through the oxidative addition of $Et_3Sn{-}H$ to **Int1′** with a free energy of −10.1 kcal/mol. These results clearly indicate that the Fe–Si bond cleavage in **R1** is much more

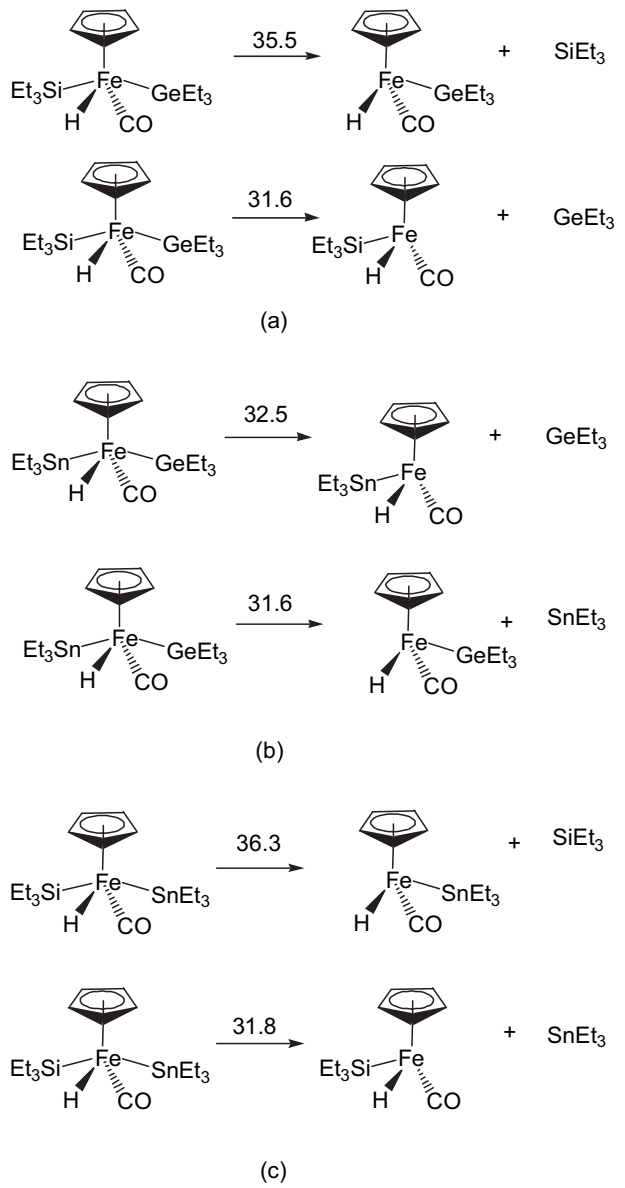

Fig. 3. Bond dissociation energies are given in kcal/mol including the basis set superposition errors (BSSE) correction using the counterpoise (CP) method.

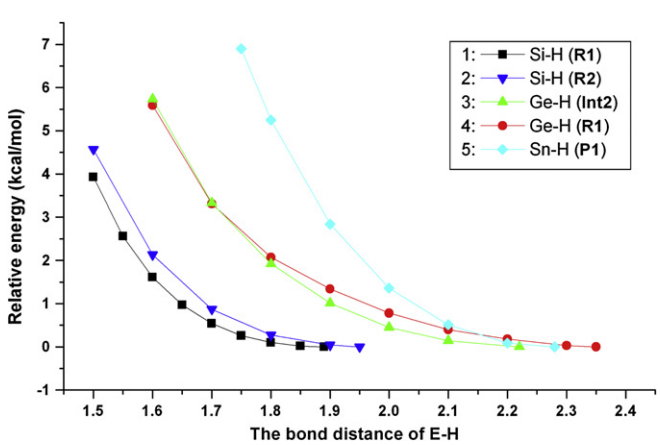

Fig. 4. Relationship between relative energies and bond distance of E–H (E = Si, Ge, Sn). The bond distance is given in Å.

thermodynamically favorable than the Fe–Ge bond cleavage in **R1**, although the Fe–Si bond is stronger than the Fe–Ge bond. That is to say, the elimination of Et_3Si–H from Fe(IV) center takes places more readily than Et_3Ge–H, which is well consistent with the experimental facts "Treatment of **R1** with a 10-fold molar excess of Et_3Sn–H for 5 min at 60 °C produced the germylstannyl complex **Int2** by the selective exchange of the Et_3Si group for the Et_3Sn group (96% NMR yield)" [32].

The second process of the ligand exchange reaction of **R1** with Et_3Sn–H is the exchange of the Et_3Ge group for the Et_3Sn group, which also undergoes two steps. The first step is the reductive elimination of Et_3Ge–H from **Int2** to give a 16e Cp(CO)Fe($SnEt_3$) (**Int3**) with a low free energy of −5.5 kcal/mol, followed by the oxidative addition of Et_3Sn–H to give a stable 18e Cp(CO)FeH($SnEt_3$)($SnEt_3$) (**P1**). The lowering of free energy difference (−8.5 kcal/mol: from **Int2** to **P1**) indicates that the process is thermodynamically favorable. The binding energies of Et_3Ge–H ($Et_3Ge + H \rightarrow Et_3Ge$–H) and Et_3Sn–H ($Et_3Sn + H \rightarrow Et_3Sn$–H) are −88.0 kcal/mol and −78.8 kcal/mol, respectively, and the Fe–Ge bond is stronger than the Fe–Sn bond (bond/dissociation energy: Fe–Ge/32.5 kcal/mol, Fe–Sn/31.6 kcal/mol, see Fig. 3(b)). In the process the reductive elimination of Et_3Ge–H from Fe(IV) center takes place more readily than Et_3Sn–H due to the thermodynamic preference and the stability of the corresponding products for the reductive elimination. The overall energy difference (from **R1** to **P1**) is −21.5 kcal/mol, indicating that the ligand exchange reaction of **R1** with Et_3Sn–H is thermodynamically favorable.

3.2. Reaction mechanisms of Cp(CO)FeH($SiEt_3$)($SnEt_3$) (R2) with Et_3Ge–H (eq. (3)) and Et_3Sn–H (eq. (4))

H. Nakazawa and co-workers also examined the reaction of silylstannyl complex **R2** with Et_3Ge–H (eq. (3)) and Et_3Sn–H (eq. (4)) to afford the corresponding complexes Cp(CO)FeH($GeEt_3$)($SnEt_3$) (**P2**) and Cp(CO)FeH($SnEt_3$)($SnEt_3$) (**P1**). The calculated free energy profiles are given in Fig. 2(c). The reactions of **R2** with Et_3Ge–H and Et_3Sn–H are proposed to undergo two steps. The first step of the two reactions is the reductive elimination of Et_3Si–H from **R2** to give a 16e Cp(CO)FeH($SnEt_3$) (**Inta**) with a low free energy of 3.8 kcal/mol. The second step is the oxidative addition of Et_3Ge–H and Et_3Sn–H to give Cp(CO)FeH($GeEt_3$)($SnEt_3$) (**P2**) and Cp(CO)FeH($SnEt_3$)($SnEt_3$) (**P1**), respectively. The lowering of energy differences (−1.8 kcal/mol from **R2** to **P2** and −11.4 kcal/mol from **R2** to **P1**) indicates the ligand exchange reactions of **R2** with $GeEt_3H$ and $SnEt_3H$ are thermodynamically favorable, in accordance with experimental results. As discussed above, Et_3Si–H instead of Et_3Sn–H in **R2** is first reductively eliminated. The bond dissociation energies of Fe–Si and Fe–Sn in **R2** are also calculated as shown in Fig. 3(c). Fe–Si bond (dissociation energy: 36.3 kcal/mol) is stronger than Fe–Sn bond (dissociation energy: 31.8 kcal/mol). Similarly, the trend is applicable to Fe(II) complexes which were reported by Koga [34]. The bond energy of Fe(II)–Si is 41.7 kcal/mol and that of Fe(II)–Sn is 36.3 kcal/mol. Further, the binding energies of the reductive products Et_3Si–H ($Et_3Si + H \rightarrow Et_3Si$–H) and Et_3Sn–H ($Et_3Sn + H \rightarrow Et_3Sn$–H) are −95.5 kcal/mol and −78.8 kcal/mol, respectively. The stable products and the thermodynamic preference make Et_3Si–H first be reductively eliminated from **R2**, although Fe–Si bond is stronger than Fe–Sn bond.

3.3. Reaction mechanisms of Cp(CO)FeH($SnEt_3$)($SnEt_3$) with Et_3Si–H and Et_3Ge–H (eq. (5))

The calculated energy profiles of Cp(CO)FeH($SnEt_3$)($SnEt_3$) (**P1**) with $SiEt_3H$ and $GeEt_3H$ are shown in Fig. 2(d), which undergo two steps, respectively. The first step is the reductive elimination of

$SnEt_3H$ to give 16e species $Cp(CO)Fe(SnEt_3)$ (**Inta**) with a high free energy of 15.2 kcal/mol, indicating the step is thermodynamically unfavorable. The second step is the oxidative addition of $SiEt_3H$ and $GeEt_3H$ to give $Cp(CO)FeH(SiEt_3)(SnEt_3)$ (**R2**) and $Cp(CO)FeH(GeEt_3)(SnEt_3)$ (**P2**), respectively. The raising of free energy differences (11.4 kcal/mol from **P1** to **R2**, 9.6 kcal/mol from **P1** to **P2**) suggests that the reactions are thermodynamically very unfavorable, which is consistent with the experimental results "a solution of the bis (stannyl) complex **P1** and a 10-fold molar excess of $Et_3E'H$(E′ = Si, Ge) was heated at 60 °C for 24 h, but the ligand exchange reaction of the Et_3Sn ligand for the Et_3E' group was not observed" [32].

From above discussion, one can see reductive elimination of Et_3Si–H from Fe(IV) complexes is the most favorable, although Fe–Si bond dissociation is more difficult than Fe–Ge bond in **R1** and Fe–Sn bond in **R2**. Si–H interaction involved in hydrido transition metal-silanes was reported [50–53]. Especially, Vyboishchikov et al. studied in 2006 the Si–H interaction in a family of silyhydride complexes $[Fe(Cp)(CO)(SiMe_nCl_{3-n}H(X))]$ (X = $SiMe_nCl_{3-n}$, H, Me, $n = 0–3$), which is similar to the compounds of Cp(CO)FeH(EEt_3)(E'Et_3) (E, E′ = Si, Ge, Sn) studied in this work, and found that the Si–H interaction was rather insensitive towards the substitution at the silicon atom and the orientation of the silyl ligand relative to the Fe–H bond [26].

We expect that the preferential reductive elimination of Et_3Si–H from **R1** and **R2** is also related to the nature of Si–H interaction. The Si–H distances are 1.89 Å in **R1** and 1.97 Å in **R2** (Fig. 1), which indicate that **R1** and **R2** belong to silylhydride complexes [53], viz. $Cp(CO)Fe(\eta^2\text{-}HSiEt_3)(GeEt_3)$ and $Cp(CO)Fe(\eta^2\text{-}HSiEt_3)(SnEt_3)$. The short bond distances suggest that strong attractive interaction can exist between silyl and hydride ligands in **R1** and **R2**. In order to prove the existence of the strong Si–H interaction we analyze the MO diagrams shown in Fig. 5 including Si–H, Ge–H and Sn–H bonds in **R1**, **R2** and **Int2**. From Fig. 5(a) we can see there is a larger overlap between Si atom and H atom than between Ge atom and H

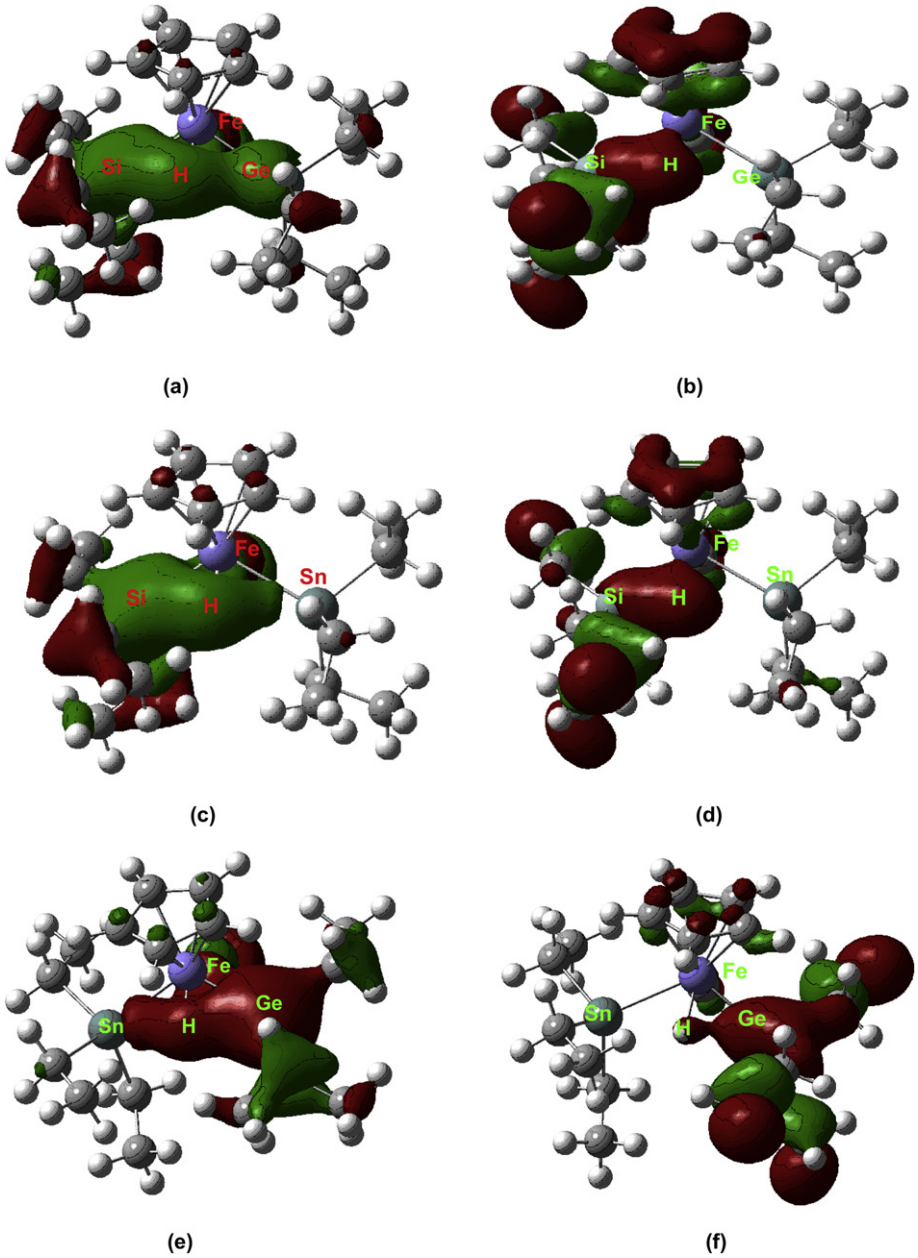

Fig. 5. Molecule orbital displays relevant to the Si–H bond, Ge–H bond and Sn–H bond in Fe–Si–Ge (**R1**), Fe–Si–Sn (**R2**) and Fe–Sn–Ge (**Int2**).

atom in **R1**. Moreover there is also an overlap between Si atom and H atom in another molecular orbital of **R1** (see Fig. 5(b)). These indicate that the interaction between Si atom and H atom in **R1** is stronger than the interaction between Ge atom and H atom in **R1**. Similarly, from Fig. 5(c) and (d) we found there also exists interaction between Si atom and H atom in **R2**, stronger than interaction between Sn atom and H atom in **R2**. The stronger interaction between Si atom and H atom further facilitates reductive elimination of $HSiEt_3$ from Fe(IV) center in **R1** and **R2**. So $HSiEt_3$ is reductively eliminated more easily than $HGeEt_3$ from **R1** and $HSnEt_3$ from **R2**. To prove the strength of the interaction of Ge–H and Sn–H. We plot the related MOs of **Int2** reflecting the Ge–H and Sn–H interactions as shown in Fig. 5(e) and 5(f). And we found that the interaction between Ge atom and H atom in **Int2** is stronger than the one between Sn atom and H atom in **Int2**, which makes $HGeEt_3$ more easily be reductively eliminated than $HSnEt_3$ from **Int2**.

4. Conclusions

The ligand exchange reaction mechanisms of $Cp(CO)FeH(EEt_3)(E'Et_3)$ with $(HEEt_3)$ (E, E′ = Si, Ge, Sn) have been investigated through DFT calculations. The reductive elimination of $HEEt_3$ from Fe(IV) center takes place more readily in the order $Et_3Si–H > Et_3Ge–H \gg Et_3Sn–H$. The reasons for the order are as follows:

(1) The thermodynamic preference for reductive elimination: $Et_3Si–H > Et_3Ge–H \gg Et_3Sn–H$.
(2) The trend of E–H binding energy: $Et_3Si–H > Et_3Ge–H > Et_3Sn–H$.
(3) The short bond distance between silyl silicon and the hydride indicates a stronger Si···H attractive interaction. The order of the interaction of E–H: $Et_3Si–H > Et_3Ge–H \gg Et_3Sn–H$.

Acknowledgment

This work was supported by the Natural Science Foundation of Shandong Province (No. Y2007B23), the State Key Laboratory of Physical Chemistry of Solid Surfaces, Xiamen University, China (No. 200702), the Key Laboratory of Colloid Interface Chemistry, Ministry of Education, Shandong University (No. 200706).

References

[1] S.J. Lippard, J.M. Berg, Principles of Bioinorganic Chemistry. University Science Books, Mill Valley, CA, 1994.
[2] I. Beletskaya, C. Moberg, Chem. Rev. 99 (1999) 3435–3462.
[3] M. Suginome, Y. Ito, Chem. Rev. 100 (2000) 3221–3256.
[4] H.K. Sharma, K.H. Pannell, Chem. Rev. 95 (1995) 1351–1374.
[5] U. Schubert, Angew. Chem. Int. Ed. 33 (1994) 419–421.
[6] C.A. Recatto, Aldrichim. Acta 28 (1995) 85–92.
[7] J.Y. Corey, J. Braddock-Wilking, Chem. Rev. 99 (1999) 175–292.
[8] Z. Lin, Chem. Soc. Rev. 31 (2002) 239–245.
[9] P. Hamon, L. Toupet, J.-R. Hamon, C. Lapinte, Organometallics 11 (1992) 1429–1431.
[10] E. Piers, R.T. Skerlj, J. Chem. Soc., Chem. Commun. 13 (1987) 1025.
[11] T.N. Mitchell, U. Schneider, B. Frohling, J. Organomet. Chem. 384 (1990) C53–C56.
[12] T. Nakano, Y. Senda, T. Miyamoto, Chem. Lett. 29 (2000) 1408–1419.
[13] Y. Senda, Y.-i. Oguchi, M. Terayama, T. Asai, T. Nakano, T. Migita, J. Organomet. Chem. 622 (2001) 302–308.
[14] T. Nakano, Y. Senda, K. Fukaya, N. Sugiuchi, S. Ni-imi, Y. Takahashi, H. Kurihara, Appl. Organomet. Chem. 19 (2005) 563–569.
[15] W. Jetz, W.A.G. Graham, J. Am. Chem. Soc. 91 (1969) 3375–3376.
[16] W. Jetz, W.A.G. Graham, Inorg. Chem. 10 (1971) 4–9.
[17] W. Jetz, W.A.G. Graham, Inorg. Chem. 10 (1971) 1159–1165.
[18] L. Manojlovic-Muir, K.W. Muir, J.A. Ibers, Inorg. Chem. 9 (1970) 447–452.
[19] R.A. Smith, M.J. Bennet, Acta Crystallogr. B33 (1977) 1118–1122.
[20] H. Brunner, K. Fisch, J. Organomet. Chem. 412 (1991) C11–C13.
[21] K. Ueno, S. Seki, H. Ogino, Chem. Lett. 12 (1993) 2159–2170.
[22] Y. Kawano, H. Tobita, H. Ogino, J. Organomet. Chem. 428 (1992) 125–143.
[23] C.L. Randolph, M.S. Wrighton, J. Am. Chem. Soc. 108 (1986) 3366–3374.
[24] K. Ueno, H. Tobita, S. Seki, H. Ogino, Chem. Lett. 22 (1993) 1723–1732.
[25] T. Sato, H. Tobita, H. Ogino, Chem. Lett. 30 (2001) 854–862.
[26] S.F. Vyboishchikov, G.I. Nikonov, Chem. Eur. J. 12 (2006) 8518–8533.
[27] M. Akita, T. Oku, M. Tanaka, Y. Moro-oka, Organometallics 10 (1991) 3080–3089.
[28] M. Akita, T. Oku, Y. Moro-oka, J. Chem. Soc., Chem. Commun. 23 (1989) 1790–1792.
[29] S. Zhang, T.L. Brown, Organometallics 11 (1992) 2122–2128.
[30] H.K. Sharma, K.H. Pannell, Organometallics 20 (2001) 7–9.
[31] C. Gordon, U. Schubert, Inorg. Chim. Acta 224 (1994) 177–179.
[32] M. Itazaki, M. Kamitani, K. Ueda, H. Nakazawa, Organometallics 38 (2009) 3601–3603.
[33] A. Guerrero, J. Cervantes, L. Velasco, J. Gomez-Lara, S. Sharma, E. Delgado, K. Pannell, J. Organomet. Chem. 464 (1994) 47–54.
[34] C.H. Suresh, N. Koga, Organometallics 20 (2001) 4333–4344.
[35] A.T. Fiedler, L.Q. Jr., Inorg. Chem. 48 (2009) 11038–11047.
[36] J.F. Berry, E. Bill, E. Bothe, F. Neese, K. Wieghardt, J. Am. Chem. Soc. 128 (2006) 13515–13528.
[37] A.D. Becke, J. Chem. Phys. 98 (1993) 5648–5652.
[38] P.J. Stephens, F.J. Devlin, C.F. Chabalowski, M.J. Fnsch, J. Phys. Chem. 98 (1994) 11623–11627.
[39] B. Michlich, A. Savin, H. Stoll, H. Preuss, Chem. Phys. Lett. 157 (1989) 200–206.
[40] C. Lee, W. Yang, R.G. Parr, Phys. Rev. B 37 (1988) 785–788.
[41] K. Fukui, J. Phys. Chem. 74 (1970) 4161–4163.
[42] K. Fukui, Acc. Chem. Res. 14 (1981) 363–368.
[43] R. Knshnan, J.S. Binkley, R. Seeger, J.A. Pople, J. Chem. Phys. 72 (1980) 650–654.
[44] P.J. Hay, W.R. Wadt, J. Chem. Phys. 82 (1985) 299–310.
[45] W.R. Wadt, P.J. Hay, J. Chem. Phys. 82 (1985) 284–298.
[46] P.C. Hariharan, J.A. Pople, Theor. Chim. Acta 28 (1973) 213–222.
[47] M.J. Frisch, et al., Gaussian 03, Revision B05. Gaussian, Inc., Pittsburgh, PA, 2003.
[48] A.A.C. Braga, G. Ujaque, F. Maseras, Organometallics 25 (2006) 3647–3658.
[49] T. Tuttle, D.Q. Wang, W. Thiel, Organometallics 25 (2006) 4504–4513.
[50] M.-F. Fan, G. Jia, Z. Lin, J. Am. Chem. Soc. 118 (1996) 9915–9921.
[51] M.-F. Fan, Z. Lin, Organometallics 16 (1997) 494–496.
[52] M.F. Fan, Z. Lin, Organometallics 18 (1999) 286–289.
[53] Z. Lin, Chem. Soc. Rev. 31 (2002) 239–245.